

Pre-Big-Bang Cosmology and Circles in the Cosmic Microwave Background

William Nelson^{1,*} and Edward Wilson-Ewing^{2,1,†}

¹*Center for Fundamental Theory, Institute for Gravitation and the Cosmos, Physics Department, Pennsylvania State University, University Park PA 16802, USA*

²*Centre de Physique Théorique de Luminy[‡], Case 907, F-13288 Marseille, EU*

We examine the possibility that circles in the cosmic microwave background could be formed by the interaction of a gravitational wave pulse emitted in some pre-big-bang phase of the universe with the last scattering surface. We derive the expected size distribution of such circles, as well as their typical ring width and (for concentric circles) angular separation. We apply these results in particular to conformal cyclic cosmology, ekpyrotic cosmology as well as loop quantum cosmology with and without inflation in order to determine how the predicted geometric properties of these circles would vary from one model to the other, and thus, if detected, could allow us to differentiate between various pre-big-bang cosmological models. We also obtain a relation between the angular ring width and the angular radius of such circles that can be used in order to determine whether or not circles observed in the cosmic microwave background are due to energetic pre-big-bang events.

PACS numbers: 98.80.Bp,98.80.Es,98.80.Qc

I. INTRODUCTION

It has recently been claimed that the Cosmic Microwave Background (CMB) exhibits circles of anomalously low temperature variance [1]. While the statistical significance of this result is in doubt [2–4] (see however [5, 6]), the intriguing possibility that such circles could be signatures of a pre-big-bang phase of our universe has been put forward [1]. The idea, originally introduced within the context of conformal cyclic cosmology [7], is that powerful events in the pre-big-bang epoch such as supermassive black hole collisions could have produced pulses of gravitational waves which would then propagate to the current post-big-bang epoch of our universe and intersect the observed CMB sphere where these pulses would leave imprints appearing as circles to observers [1, 7].

More specifically, if a cosmological model allows a pre-big-bang epoch during which the universe is large and classical, it could be populated by galaxies, stars and black holes just as it is today and, in particular, it would be possible for collisions between supermassive black holes to occur. Such a collision would release a brief, intense gravitational wave pulse that would expand radially at the speed of light. This pulse would travel through the transition between the pre- and post-big-bang phases and continue expanding in our current post-big-

[‡] Unité mixte de recherche (UMR 6207) du CNRS et des Universités de Provence (Aix-Marseille I), de la Méditerranée (Aix-Marseille II) et du Sud (Toulon-Var); laboratoire affilié à la FRUMAM (FR 2291).

*Electronic address: nelson@gravity.psu.edu

†Electronic address: wilson-ewing@cpt.univ-mrs.fr

bang epoch and could potentially be observed by future gravitational wave detectors. In addition, it has been suggested that this pulse could leave an imprint on the last scattering surface (LSS). This imprint could be detected as the temperature variance on the surface of the pulse sphere would be slightly lower than average since the pulse would homogenise the electromagnetic matter field and thus ensure that the temperature is more highly correlated on the pulse sphere than elsewhere [1, 7]. Finally, if this sphere with an anomalously low temperature variance intersects the observed CMB sphere, it would appear to us as a circle in the CMB.

Even though such a scenario is rather speculative, the possibility that information from a previous phase of cosmology can be gleaned from the CMB is an exciting one. Note that even if there are strong gravitational wave pulses coming from a pre-big-bang epoch that interact with the CMB (which is already a strong assumption), it is not clear what mechanism would allow these pulses to leave an imprint on the CMB. Indeed the standard Sachs-Wolfe effect would simply change the average CMB temperature of the rings¹ (rather than the variance) [8] and hence some entirely new mechanism would be required in order for the pulses to leave an imprint of type reported in [1, 7].

Nonetheless, if such circles are indeed found, their properties would depend on the dynamics of the pre-big-bang era of the universe and therefore different cosmological models would predict different properties for circles in the CMB. For example, if in one cosmology black hole collisions are expected to occur close to the transition between the pre- and post-big-bang epochs, the gravitational wave pulse sphere will not have much time to expand and therefore would be smaller in this cosmology than in a different model where the gravitational wave pulse has a longer time to expand before it reaches the last scattering surface. This is one example of a difference between various cosmological models that will have an effect on the geometric properties of any circles in the CMB. The goal of this paper is to determine some of the properties of these circles that depend on the pre-big-bang cosmology, should conclusive observations be made.

The outline of the paper is as follows: in Sec. II we study the basic properties of the gravitational wave sphere produced by a supermassive black hole collision and also the CMB sphere seen today. In Sec. III, we derive some relations between geometric characteristics of the circles —specifically their size, their width and the separation between concentric circles— and the properties of the spheres studied in Sec. II. Then in Sec. IV we consider four specific cosmological models which each have a pre-big-bang epoch: conformal cyclic cosmology, ekpyrotic cosmology and loop quantum cosmology with and without inflation. We use the results of Sec. III in order to determine what circles in the CMB would appear like for each model. We end with a discussion in Sec. V.

II. THE TWO INTERSECTING SPHERES

In order for there to be a circular imprint in the CMB, we first assume that an extremely energetic event occurs in the pre-big-bang epoch and releases a strong pulse of gravitational radiation. This pulse forms an expanding sphere which propagates to the current post-

¹ Note that the results presented in this work concerning the geometric properties of the circles are also applicable to rings that have an anomalously high or low average temperature. However, there is currently no observational data suggesting that such rings exist.

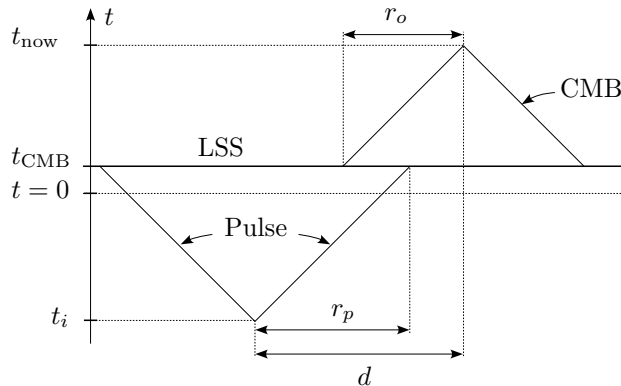


FIG. 1: The conformal diagram of the expanding (null) pulse, intersecting the last scattering surface (LSS). The CMB sphere as seen today is also pictured. The time $t = 0$ corresponds to the transition between the pre-big-bang and post-big-bang epochs. The detailed dynamics near the transition point are of course model-specific.

big-bang era and eventually reaches the LSS. To us the LSS appears to be a sphere, with the Earth at the centre, simply because it occurred at the same time everywhere due to homogeneity and the light travelled equal distances in each direction due to the isotropic expansion of the universe. Thus when the two spheres corresponding to the gravitational wave pulse and the observed CMB intersect, the result is a circle. See Fig. 1 for a conformal diagram showing the intersection of these two spheres.

The interaction of the pulse with the recombination process taking place at the LSS is then assumed to affect the plasma on these circles in some way which homogenises the temperature, and this as yet unknown mechanism will then produce circles of abnormally low temperature variance in the CMB which could potentially be observed [7].

We will now determine some of the relevant properties of the gravitational wave pulse sphere and the observed CMB sphere.

A. Some Properties of the Intersecting Spheres

Assuming homogeneity and isotropy as well as spatial flatness gives the flat Friedmann-Lemaître-Robertson-Walker (FLRW) space-time whose line element is given by

$$ds^2 = -c^2 dt^2 + a^2(t) \left[dr^2 + r^2 d\Omega^2 \right], \quad (2.1)$$

where t is the proper time and we will normalise the scale factor so that $a(t_{\text{now}}) = 1$ where t_{now} is the proper time today. Observations indicate that recombination occurred approximately 380 000 years after the beginning of the current era of the universe [9], or

$$t_{\text{CMB}} \approx 10^{56} t_{\text{Pl}}, \quad (2.2)$$

where we have set $t = 0$ to be the beginning of the current epoch of the universe. One can also show that the energy density at recombination is of the order of

$$\rho_{\text{CMB}} := \rho(t_{\text{CMB}}) \approx 10^{-115} \rho_{\text{Pl}}. \quad (2.3)$$

Finally, since we have chosen $a(t_{\text{now}}) = 1$, we also find that

$$a(t_{\text{CMB}}) \approx 1089^{-1}. \quad (2.4)$$

See, e.g., [9] for further background information about the standard cosmological picture.

From (2.1), it follows that the trajectory of a (null) radial gravitational wave pulse will be given by

$$c \frac{dt}{a(t)} = dr. \quad (2.5)$$

Therefore, the coordinate radius $r_p(t_f)$ of a gravitational wave sphere which left a central point at t_i (e.g., due to a supermassive black hole collision occurring at t_i) is given by

$$r_p(t_f) = c \int_{t_i}^{t_f} \frac{dt}{a(t)}. \quad (2.6)$$

Since the scale factor $a(t)$ is by definition positive, it follows that r_p grows with time as one would expect. Note that we shall use a lower case r to denote coordinate radii and an upper case R for physical radii. The physical radius of the pulse sphere is simply given by

$$R_p(t_f) = a(t_f) r_p(t_f). \quad (2.7)$$

As $a(t_{\text{now}}) = 1$, it follows that today the physical and coordinate distances coincide.

The coordinate and physical radii of a gravitational pulse due to an event which occurred at the time t_i , when recombination occurs, is then given by

$$r_p := r_p(t_{\text{CMB}}) = c \int_{t_i}^{t_{\text{CMB}}} \frac{dt}{a(t)}, \quad R_p(t_{\text{CMB}}) = a(t_{\text{CMB}}) r_p. \quad (2.8)$$

Similarly, the coordinate and physical radii of the CMB sphere as seen by an observer today are

$$r_o := r_o(t_{\text{now}}) = R_o(t_{\text{now}}) = c \int_{t_{\text{CMB}}}^{t_{\text{now}}} \frac{dt}{a(t)}. \quad (2.9)$$

It is possible to obtain a value for r_o by using the Friedmann equation

$$H^2 = \frac{8\pi G}{3} \left[\frac{\rho_m|_0}{a^3} + \frac{\rho_\gamma|_0}{a^4} + \rho_\Lambda \right], \quad (2.10)$$

from which, using the Λ CDM parameters with $\rho_m|_0 \approx 2.12 \times 10^{-30} \text{ g cm}^{-3}$ the (cold dark) matter density today, $\rho_\gamma|_0 \approx 7.8 \times 10^{-34} \text{ g cm}^{-3}$ the radiation density today and the energy density due to the nonzero cosmological constant being $\rho_\Lambda \approx 1.4 \times 10^{-29} \text{ g cm}^{-3}$ (see, e.g., [10] for details), one finds that

$$\dot{a} \approx 2 \times 10^{-20} \left[\frac{1}{a^2} + \frac{2700}{a} + 18000a^2 \right]^{1/2} \text{ s}^{-1}. \quad (2.11)$$

Equation (2.9), rewritten in the form

$$r_o = c \int_{a(t_{\text{CMB}})}^{a(t_{\text{now}})} \frac{1}{a} \frac{dt}{da} da, \quad (2.12)$$

can be evaluated by using (2.11) and numerically integrating between $a(t_{\text{CMB}}) \approx 1089^{-1}$ and $a(t_{\text{now}}) = 1$. This gives the result

$$r_o \approx 3 \times 10^{61} \ell_{\text{Pl}} . \quad (2.13)$$

A final point is that recombination does not occur instantaneously but occurs over a finite amount of time (between scale factors given by $a = (1089 \pm 195)^{-1}$ [10]) and thus the last scattering surface has a thickness of

$$\delta r_o \approx 3 \times 10^{59} \ell_{\text{Pl}} . \quad (2.14)$$

The value of r_o and its thickness are both well known and will not change from one pre-big-bang cosmological model to another. However, $a(t_i)$ and r_p both strongly depend upon the cosmology. This dependence of $a(t_i)$ and r_p on the cosmological model will in turn have an effect on the properties of any circles in the CMB. This is what we shall quantify in Sec. III before performing some case studies in Sec. IV. However, we will first examine some important geometric relations between the intersecting gravitational pulse sphere and the CMB sphere with the resulting circle.

B. Geometric Relations Between the Spheres and the Resulting Circle

We will use the indices p for the pulse sphere and o for the observed CMB sphere. Finally, θ_p will denote the angular radius of the circle as seen from the centre of the gravitational wave pulse while θ_o will denote the circle's angular radius as seen by us, the observers. Note that these angles are defined as the angular distance from a point on the circumference of the circle to the centre of the circle. Since the angles θ_i are a measure of the radius of a circle rather than its diameter, it follows that $\theta_i \in (0, \frac{\pi}{2})$.

It is immediately clear that

$$r_c = r_o \sin \theta_o = r_p \sin \theta_p , \quad (2.15)$$

and also that the coordinate separation d between the centres of the pulse sphere and the CMB sphere is given by

$$d = r_p \cos \theta_p + r_o \cos \theta_o . \quad (2.16)$$

Finally, by the cosine law it follows that

$$\cos \theta_o = \frac{r_o^2 - r_p^2 + d^2}{2r_o d} . \quad (2.17)$$

Note that if $r_p > r_o$, it is possible for $\cos \theta_o$ to be negative and therefore for $\theta_o > \frac{\pi}{2}$. However, the angular radius of such a circle would in fact be given by $\pi - \theta_o$. In order to incorporate this effect, it is sufficient to change the above expression to

$$\cos \theta_o = \frac{|r_o^2 - r_p^2 + d^2|}{2r_o d} , \quad (2.18)$$

and now $0 \leq \theta_o \leq \frac{\pi}{2}$ as desired. Note that while this expression holds for each circle, r_p and d will of course vary from circle to circle.

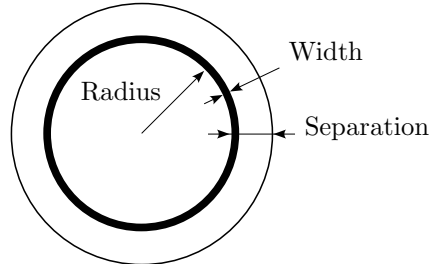


FIG. 2: The geometric properties of the circles we are interested in: their angular radius (Sec. III A), the typical angular separation between concentric circles (Sec. III B) and the angular ring width of the circles (Sec. III C).

III. EXPECTED CHARACTERISTICS OF THE CIRCLES

Here we will use the relations obtained in the previous section in order to determine, for a given $a(t_i)$ and r_p , some of the characteristics we expect the circles to have. In particular, we will determine the expected size of the circles (in terms of their angular radius), the typical angular separation between concentric circles and also the angular ring width of the circles (see Fig. 2). This will allow us to quantify how the geometric properties of the circles vary when (the cosmological model and hence) $a(t_i)$ and r_p change.

A. The Size of the Circles

Given r_p and d , one can use (2.18) to determine the angular size of the circle. While estimates for r_p can be obtained for each cosmology (see Sec. IV for some examples), d is not an observable. Since d cannot be measured, it is impossible to use (2.18) to predict the size of a specific circle and hence what would actually be observed in the CMB. However, it can be used in order to obtain the *probability distribution* of the size of the circles, which could then be compared to observations in order to constrain the pre-big-bang cosmological model.

If we assume that the events that caused the gravitational wave pulses, e.g., supermassive black hole collisions, are spread out in an approximately random fashion throughout the universe, then we can treat d as an essentially stochastic variable. Then the expectation value for d is given by

$$\langle d \rangle = \left[\int_0^{4\pi} d\Omega \int_{d_{min}}^{d_{max}} dd d^2 \cdot d \right] \times \left[\int_0^{4\pi} d\Omega \int_{d_{min}}^{d_{max}} dd d^2 \right]^{-1}, \quad (3.1)$$

where d_{min} and d_{max} are easily determined as the gravitational wave pulse sphere and the CMB sphere will only intersect if

$$|r_p - r_o| \leq d \leq r_p + r_o, \quad (3.2)$$

and in the extreme cases the spheres only intersect at a point (see Fig. 1).

However, since d cannot be measured, $\langle d \rangle$ is not a very useful quantity to know. Rather, we are interested in calculating the angular size of the circles in the CMB. Using (2.18), it

can be seen that

$$\langle \theta_o \rangle = \left[\int_0^{4\pi} d\Omega \int_{|r_p-r_o|}^{r_p+r_o} dd d^2 \cdot \theta_o(d) \right] \times \left[\int_0^{4\pi} d\Omega \int_{|r_p-r_o|}^{r_p+r_o} dd d^2 \right]^{-1}, \quad (3.3)$$

where

$$\theta_o(d) = \cos^{-1} \left(\frac{|r_o^2 - r_p^2 + d^2|}{2r_o d} \right), \quad (3.4)$$

and now it is possible to determine the expected size of the circles in the CMB if r_p is known.

It is also straightforward to calculate the variance,

$$\sigma_{\theta_o}^2 = \langle \theta_o^2 \rangle - \langle \theta_o \rangle^2, \quad (3.5)$$

where, as usual,

$$\langle \theta_o^2 \rangle = \left[\int_0^{4\pi} d\Omega \int_{|r_p-r_o|}^{r_p+r_o} dd d^2 \cdot \theta_o^2(d) \right] \times \left[\int_0^{4\pi} d\Omega \int_{|r_p-r_o|}^{r_p+r_o} dd d^2 \right]^{-1}. \quad (3.6)$$

With these equations, we can predict the distribution of the size of the circles in the CMB for a given cosmological model.

1. The $r_p \gg r_o$ Limit

Consider first the $r_p \gg r_o$ case, in which case $d \in (r_p - r_o, r_p + r_o)$ and d can be parametrised as

$$d = r_p + \ell r_o, \quad (3.7)$$

where $\ell \in (-1, 1)$.

We can now evaluate the expected mean value of θ_o ,

$$\langle \theta_o \rangle = \frac{\int_{-1}^1 d\ell r_o r_p^2 (1 + 2\frac{r_o}{r_p}\ell + \frac{r_o^2}{r_p^2}\ell^2) \theta_o(\ell)}{2r_p^2 r_o \left(1 + \frac{r_o^2}{3r_p^2}\right)}, \quad (3.8)$$

where

$$\theta_o(\ell) = \cos^{-1} \left[\left| \ell + \frac{r_o}{2r_p} (1 - \ell^2) - \frac{r_o^2}{2r_p^2} \ell (1 - \ell^2) + O\left(\frac{r_o^3}{r_p^3}\right) \right| \right], \quad (3.9)$$

and Taylor expansions have been used on the right hand side in order to obtain a polynomial in $\frac{r_o}{r_p}$ inside the inverse cosine. We can further simplify the equation by expanding the inverse cosine itself around the point ℓ . However, one cannot use the naïve Taylor expansion as it fails near $\ell \approx -r_o/2r_p$ when the argument of the inverse cosine is zero as the absolute value function is not differentiable at zero. In order to avoid this problem, we will use two separate expansions: one for the region where ℓ is of the order of r_o/r_p and another elsewhere.

More precisely, for $\ell \in (-r_o/r_p, r_o/r_p)$, we find

$$\theta_o(\ell) = \frac{\pi}{2} - \left| \ell + \frac{r_o}{2r_p} \right| + O\left(\frac{r_o^3}{r_p^3}\right), \quad (3.10)$$

while for all other ℓ

$$\theta_o(\ell) = \cos^{-1} |\ell| - \frac{r_o}{2r_p} \text{sgn}(\ell) \sqrt{1 - \ell^2} + \frac{3r_o^2}{8r_p^2} |\ell| \sqrt{1 - \ell^2} + O\left(\frac{r_o^3}{r_p^3}\right). \quad (3.11)$$

Note that both expansions agree at the points $\ell = \pm r_o/r_p$, at least up to order r_o^3/r_p^3 . These expressions are both easily integrated and one finds that

$$\langle \theta_o \rangle = 1 - \frac{4r_o^2}{9r_p^2} + O\left(\frac{r_o^3}{r_p^3}\right). \quad (3.12)$$

This shows that the average angular radius for circles in the limiting case $r_p \gg r_o$ will be 1 rad or 57° . In order to determine the variance we must also calculate $\langle \theta_o^2 \rangle$, once more using (3.10) and (3.11), and after a tedious but straightforward calculation one finds

$$\langle \theta_o^2 \rangle = \pi - 2 - \frac{4}{27} (3\pi - 4) \frac{r_o^2}{r_p^2} + O\left(\frac{r_o^3}{r_p^3}\right), \quad (3.13)$$

and therefore the variance is

$$\sigma_{\theta_o}^2 = \pi - 3 - \frac{4}{27} (3\pi - 10) \frac{r_o^2}{r_p^2} + O\left(\frac{r_o^3}{r_p^3}\right). \quad (3.14)$$

Therefore, for cosmological models where $r_p \gg r_o$, although the variance is relatively high, it is clear that the average value of θ_o would be near 57° and most θ_o would be in the interval $(35^\circ, 79^\circ)$.

2. The $r_p = r_o$ Case

One can also consider the case where $r_p = r_o$, in which case

$$\theta_o(d) = \cos^{-1} \left(\frac{d}{2r_o} \right), \quad (3.15)$$

and then it follows that

$$\langle \theta_o \rangle = \frac{2}{3} \approx 38^\circ, \quad (3.16)$$

while

$$\langle \theta_o^2 \rangle = \frac{6\pi - 14}{9} \approx (42^\circ)^2, \quad (3.17)$$

and this gives a variance of

$$\sigma_{\theta_o}^2 = \frac{2\pi - 6}{3} \approx (18^\circ)^2. \quad (3.18)$$

The expected variance is relatively large, but it is nonetheless clear that typical circles in the CMB would be quite large (i.e., greater than $\approx 20^\circ$) for the $r_p \approx r_o$ case.

3. The $r_p \ll r_o$ Limit

As the last limiting case, we will consider the situation where $r_p \ll r_o$. We can again parametrise d , this time as

$$d = r_o + \ell r_p, \quad (3.19)$$

where $\ell \in (-1, 1)$.

In this situation

$$\theta_o = \cos^{-1} \left[\frac{1 + \ell \frac{r_p}{r_o} - \frac{1}{2} (1 - \ell^2) \frac{r_p^2}{r_o^2}}{1 + \ell \frac{r_p}{r_o}} \right] = \cos^{-1} \left[1 - \frac{\frac{1}{2} (1 - \ell^2) \frac{r_p^2}{r_o^2}}{1 + \ell \frac{r_p}{r_o}} \right], \quad (3.20)$$

and using the expansion $\cos^{-1}(1 - x) \approx \sqrt{2x} + O(x^{3/2})$, we can expand to get

$$\theta_o = \sqrt{1 - \ell^2} \frac{r_p}{r_o} \left[1 - \frac{\ell r_p}{2r_o} + O\left(\frac{r_p^2}{r_o^2}\right) \right]. \quad (3.21)$$

With this expression for θ_o , it is easy to calculate that

$$\langle \theta_o \rangle = \frac{\pi r_p}{4r_o} + O\left(\frac{r_p^3}{r_o^3}\right), \quad (3.22)$$

and

$$\langle \theta_o^2 \rangle = \frac{2r_p^2}{3r_o^2} + O\left(\frac{r_p^4}{r_o^4}\right). \quad (3.23)$$

It then follows that the variance is

$$\sigma_{\theta_o}^2 = \left(\frac{2}{3} - \frac{\pi^2}{16} \right) \frac{r_p^2}{r_o^2} + O\left(\frac{r_p^4}{r_o^4}\right). \quad (3.24)$$

A final important point is that the maximal angular radius θ_o^{\max} possible in this case is

$$\theta_o^{\max} = \sin^{-1} \left(\frac{r_p}{r_o} \right) = \frac{r_p}{r_o} + O\left(\frac{r_p^3}{r_o^3}\right); \quad (3.25)$$

clearly, one of the principle signatures of the $r_p \ll r_o$ limit is the presence of *only* very small circles.

4. Further Remarks

After the study of these three limiting scenarios, it is clear that it is only for cosmological models where r_p is smaller than r_o that one would *a priori* expect to see more small circles in the CMB than large ones. In all other cases the majority of the circles observed in the CMB should be quite large, with an angular radius approximately in the range of $\theta_o \in (20^\circ, 90^\circ)$.

Nonetheless, there may be some selection effects which come into play. For example, it may be hard to see very large circles as they would necessarily cross the equatorial plane in the CMB and therefore significant portions of these circles would be masked by the foreground. It is also possible that there are some other effects which make smaller circles easier to detect (one such effect is presented in Sec. III C). Still, unless these selection effects are very strong, the results found in the three limiting cases studied here can be very useful, as we shall see in Sec. IV.

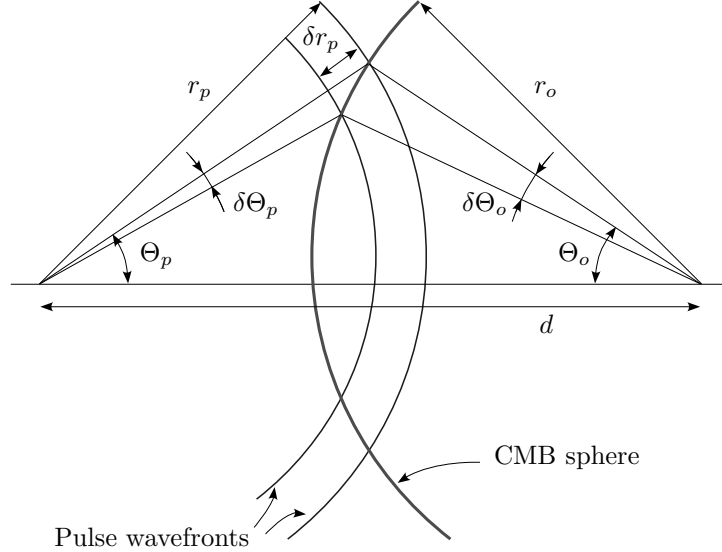


FIG. 3: A pair of spherical pulses with coordinate radii r_p and $r_p - \delta r_p$, intersecting the observed CMB sphere of radius r_o .

B. Separation Between Concentric Circles

It has been pointed out that if there are repeated emissions from one particular source (e.g., a supermassive black hole that collides with several other large black holes over time), this would result in concentric circles [1, 7]. The angular separation between such concentric circles would depend on the angular radius of the observed circles and the distance to the source as well as the original frequency of the source.

For simplicity, we will assume recombination to have occurred instantaneously, leading to a thin CMB surface (one can generalise the results presented here by following similar arguments). Let us consider two concentric pulse spheres, of coordinate radii r_p and $r_p - \delta r_p$, where δr_p is the coordinate distance between the two gravitational wave pulses.

Using the conventions shown in Fig. 3, we can apply Eq. (2.18) to the larger and smaller concentric circles and this gives, respectively,

$$\cos \theta_o = \frac{|r_o^2 - r_p^2 + d^2|}{2r_o d}, \quad (3.26)$$

$$\cos (\theta_o - \delta \theta_o) = \frac{|r_o^2 - (r_p - \delta r_p)^2 + d^2|}{2r_o d}. \quad (3.27)$$

Combining these equations gives

$$\frac{\delta r_p (2r_p - \delta r_p)}{2r_o d} = \cos (\theta_o - \delta \theta_o) - \cos (\theta_o), \quad (3.28)$$

where for the sake of simplicity we have assumed that $r_o^2 - r_p^2 + d^2 > 0$. Note that since the time elapsed between two separate gravitational wave pulses can be significant, we cannot assume that δr_p and $\delta \theta_o$ are small². If $r_o^2 - r_p^2 + d^2 < 0$, then the resulting equation will be

² Although one cannot assume δr_p or $\delta \theta_o$ to be small in generic situations, there are some cases where (3.28)

a little more complicated as the absolute value signs cannot be removed.

Following (2.6), we also find that the coordinate separation δr_p between two separate pulses is given by

$$\delta r_p = c \int_{t_1}^{t_2} \frac{dt}{a(t)}, \quad (3.29)$$

where t_1 and t_2 are the (proper) times when, respectively, the first and second pulses were emitted.

In general, if there are a large number of circles observed in the CMB, one can use this data to try to fit (3.28) in order to determine typical values of both δr_p and r_p . This could provide some information on the pre-big-bang epoch, in particular regarding the frequency of supermassive black hole collisions in that era.

C. The Width of the Circles

It is also possible to obtain some information regarding the widths of the circles. If the cause of the circles is a pulse of gravitational waves intersecting the last scattering surface, then the pulse width would result in some characteristic width of the observed circles.

It is possible to use the same setup as in the previous section, where now the two waves in Fig. 3 correspond to the leading trailing wave-fronts of the same gravitational wave pulse, rather than two separate pulses, and δ corresponds to the coordinate thickness of the pulse while $\delta\theta_o$ gives the width of the circle.

It is also necessary to take the width δr_o of the CMB sphere into account. This situation can be described by a diagram similar to that given in Fig. 3 except that the CMB sphere on the right also has a width: the outer radius is given by r_o , while the inner radius is $r_o - \delta r_o$.

A careful analysis shows that, depending on the situation, the relevant intersections are either the r_o and $r_p - \delta r_p$ intersection and the $r_o - \delta r_o$ and δr_p intersection or else the r_o and r_p intersection and the $r_o - \delta r_o$ and $r_p - \delta r_p$ intersection³. We will begin by considering the first case.

Using the cosine rule for the first two intersections described above, we find that

$$\cos(\theta_o) = \frac{d^2 + (r_o - \delta r_o)^2 - r_p^2}{2(r_o - \delta r_o)d}, \quad (3.30)$$

$$\cos(\theta_o - \delta\theta_o) = \frac{d^2 + r_o^2 - (r_p - \delta r_p)^2}{2r_o d}. \quad (3.31)$$

Since we expect the width of the circles to be quite small (say less than 1°), we can restrict our attention to $\delta\theta_o \ll \theta_o$ and $\delta \ll r_p$ (we already know that $\delta r_o/r_o \approx 0.01$). Therefore, we can solve for $\delta\theta_o$ by taking the difference between these two equations and only keeping terms that are linear in δr_o , δr_p and $\delta\theta_o$. This gives

$$\delta\theta_o \sin \theta_o = \frac{r_p}{r_o d} \delta r_p + \frac{r_p^2 + r_o^2 - d^2}{2r_o^2 d} \delta r_o. \quad (3.32)$$

can be simplified. For example, if certain cosmological scenarios decree that $r_p \ll r_o$, it follows that δr_p , being smaller than r_p , is also much smaller than r_o and also that $d \approx r_o$. In this limit, $\delta\theta_o < \theta_o \ll 1$ and, by using several Taylor expansions, one can show that (3.28) becomes $\delta r_p \approx (r_o^2/r_p) \cdot \delta\theta_o \sin \theta_o$.

³ We would like to thank Alexey Bobrick for pointing this out.

It is easy to study the other case as well and it can be incorporated by changing the relation above to⁴

$$\delta\theta_o \sin\theta_o = \frac{r_p}{r_o d} \delta r_p + \frac{|r_p^2 + r_o^2 - d^2|}{2r_o^2 d} \delta r_o. \quad (3.33)$$

Note that since $\theta_o > \theta_o - \delta > 0$, it follows that θ_o is strictly greater than zero and therefore $\sin\theta_o > 0$. The width of the circles seen in the CMB comes from two contributions: the width of the gravitational pulse δr_p and the width of the CMB sphere δr_o given in (2.14). Since δr_o is already known, the remaining task is to determine δr_p .

If the circles observed in the CMB were to come from an event which has a typical time-scale δt , then assuming that the scale factor is approximately constant during this event⁵

$$\delta r_p = c \int_{t_i}^{t_i + \delta t} \frac{dt}{a(t)} \approx \frac{c \delta t}{a(t_i)}, \quad (3.34)$$

where we have made the approximation that the scale factor is approximately constant in the interval $(t_i, t_i + \delta t)$. This gives

$$\delta\theta_o = \frac{r_p}{r_o d \sin\theta_o} \frac{c \delta t}{a(t_i)} + \frac{|r_p^2 + r_o^2 - d^2|}{200 r_o d \sin\theta_o}, \quad (3.35)$$

where we have used that $\delta r_o/r_o = 1/100$.

As a specific example, consider the collision of supermassive black holes. In this case, the distance between the leading and trailing wave fronts should be of the same order as the length of the ‘‘chirp’’ gravitational wave burst that occurs at the end of the merger of two black holes. The physical time scale of the chirp in proper time coordinates is typically of the order of a few days, i.e., $\delta t \sim 8.6 \times 10^4$ s (the time scale may change depending upon the exact type of event in which case one would have to modify the following relations accordingly). Therefore,

$$\delta r_p \approx \frac{2 \times 10^{48} \ell_{\text{Pl}}}{a(t_i)}, \quad (3.36)$$

where $a(t_i)$ is the scale factor of the universe when the black holes merge. From (2.14), it follows that, unless $a(t_i) \leq 10^{-11}$ or the coefficient of δr_p is larger than that of δr_o by several orders of magnitude, the contribution due to δr_p is completely negligible compared to that due to δr_o in which case

$$\delta\theta_o \approx \frac{|r_p^2 + r_o^2 - d^2|}{2r_o^2 d \sin\theta_o} \delta r_o \approx \frac{|r_p^2 + r_o^2 - d^2|}{200 r_o d \sin\theta_o}. \quad (3.37)$$

One can solve for d in terms of r_o, r_p and θ_o by using (2.15) and (2.16), but that will not be necessary for our purposes here.

⁴ By considering these two cases, we obtain this relation which holds for both positive and negative $r_o^2 - r_p^2 + d^2$ so long as we use conventions where $0 < \theta_o - \delta\theta_o < \theta < \frac{\pi}{2}$.

⁵ An effect that has been neglected in this analysis is the fact that the gravitational wavefront will spread as different wavelengths will travel at different speeds through various matter fields. Although this effect is completely negligible when the matter energy density is low, it could become important as the Planck scale is approached and the electromagnetic and then the quark-gluon plasmas are formed. This would contribute to a slightly larger δr_p .

In order for a circle to be observed by the WMAP and/or Planck satellites, its width must be at least as large as the angular resolution of the satellites which is of the order of 0.25° . Clearly, in some cosmological scenarios the width should be observable, while in others it might not be.

We can also see that it is easier to detect smaller circles due to the denominator of $\sin \theta_o$. Indeed, the denominator of $\sin \theta_o$ provides a significant selection effect whereby smaller circles will be thicker and therefore easier to detect. Therefore, even if the typical circle size for a given cosmological model is quite large, small circles could be the first ones observed as their width is the largest. Assuming circles are detected in the CMB with sufficient resolution, it should be possible to detect this variation in the width with respect to the angular size of the circles⁶.

As a final remark, we point out that if $\delta\theta_o \geq 5^\circ$, the approximation that lead to (3.33) breaks down. In this case, one would have to keep all of the higher order terms that were neglected in this analysis in order to determine the relation between the thickness of the pulse and the width of the circle.

IV. EXAMPLES: SPECIFIC PRE-BIG-BANG COSMOLOGICAL MODELS

Now we will consider four specific pre-big-bang cosmological models in order to determine how the properties of circles appearing in the CMB vary from one model to another. Specifically, we will derive typical values of $a(t_i)$ and r_p for each cosmology and determine in turn what circle size and width are to be expected in each case.

We will begin by considering conformal cyclic cosmology (CCC) where it was first pointed out that gravitational waves from a pre-big-bang eon might leave circular imprints in the CMB. We will then go on to consider three other cosmological models which also have a pre-big-bang branch and hence could also provide a similar mechanism that would lead to circles in the CMB. These models are the ekpyrotic universe as well as loop quantum cosmology (LQC), both with and without slow-roll inflation after the bounce.

It is important to point out that much more work is needed in order to say that any of these cosmological models necessarily predicts the presence of circles in the CMB. In particular, one would need to understand how the perturbations in the gravitational field will be transferred to the CMB and how strong this effect will be. It is quite possible that this effect will be very small and that therefore it will be impossible to detect, even if it is indeed present. One would also need to have a fully developed, non-singular theory in order to describe how these perturbations propagated from the pre- to post-big-bang epochs. For example, although general symmetry arguments may be sufficient to predict that the pulses remain spherical through the transition (at least assuming cosmological anisotropies remain small), only a full understanding of the underlying theory would allow us to predict that such transitions even occur. Thus, the presence of circles in the CMB is a signature of a pre-big-bang cosmological scenario rather than a prediction of them.

Nonetheless, if such circles are observed, their properties would provide information about the pre-big-bang phase, in particular regarding the typical values of r_p , which is related to

⁶ Note that there is an additional dependence on θ_o in d as $d = r_o \cos \theta_o + \sqrt{r_p^2 - r_o^2 \sin^2 \theta_o}$. However, so long as r_o and r_p are of different orders of magnitude, this additional dependence on θ_o will be sub-leading.

the average size of the circles, and $a(t_i)$, which can affect the width of the circles. This would, in principle, allow us to differentiate between different pre-big-bang cosmological models.

A. Conformal Cyclic Cosmology

Conformal cyclic cosmology (CCC) was first introduced by Penrose and the basic idea is that the universe, when the scale factor diverges to infinity, is conformally mapped to a space-time where the scale factor is zero and hence to another big bang at which point a new epoch begins [7]. Due to the presence of a nonzero cosmological constant, the scale factor of the universe diverges in a finite amount of conformal time and therefore there are an infinite number of epochs: each new epoch begins with a big bang when the infinite scale factor of the previous epoch is conformally mapped to zero.

There is an ambiguity in how this mapping is done which is still not fully understood (see, e.g., Sec. B10 in [7]) and here we will choose a conformal mapping where the coordinate distance (and therefore also the comoving distance) between any two points remains constant during the transition from one epoch to the next. This is a conformal mapping with nice properties, but it is one possibility out of a one-parameter family of allowed conformal mappings. For this section, we will focus on the mapping chosen here and we will comment at the end on other possible choices.

In the CCC paradigm, the most powerful supermassive black hole collisions would happen at very late times in each epoch and thus $a(t_i) > a(t_{\text{now}}) = 1$. Such a scale factor at the black hole collision time indicates that the width of the circles is dominated by the thickness of the CMB sphere [see (2.14), (3.35) and (3.36)] and therefore Eq. (3.37) holds and can be used to relate the width of a given circle to r_o, r_p and its angular radius.

It is possible to bound r_p ,

$$r_p = \int_{t_i}^{t_{\text{CMB}}} \frac{dt}{a(t)}, \quad (4.1)$$

by determining the behaviour of $a(t)$ in each epoch. At first, when the pulse occurs, the universe's dynamics are dominated by the cosmological constant $\Lambda \approx 3.3 \times 10^{-122} \ell_{\text{Pl}}^{-2}$ [10] and therefore, for $t \in (t_i, +\infty)$,

$$a(t) = \exp(Ht), \quad (4.2)$$

where the Hubble rate is $H = \sqrt{\Lambda/3}$.

For the next epoch, there is no inflation after the big bang and we will assume that the universe is radiation-dominated, at least until recombination, in which case we have the relation

$$\rho = \frac{\rho_o}{a(t)^4}, \quad (4.3)$$

where ρ_o is determined by some initial conditions. From (2.3) and (2.4), one can see that

$$\rho_o \approx 10^{-127} \rho_{\text{Pl}}, \quad (4.4)$$

and then by solving Einstein's equations, one finds that for $t \in (0, t_{\text{CMB}})$

$$a(t) = \left(\frac{32\pi G \rho_o}{3} \right)^{1/4} \sqrt{t}. \quad (4.5)$$

It follows that

$$\begin{aligned} r_p &= \int_{t_i}^{+\infty} \frac{dt}{e^{Ht}} + \left(\frac{3}{32\pi G\rho_o} \right)^{1/4} \int_0^{t_{\text{CMB}}} \frac{dt}{\sqrt{t}} \\ &= \frac{1}{a(t_i)H} + \left(\frac{3}{2\pi G\rho_o} \right)^{1/4} \sqrt{t_{\text{CMB}}} . \end{aligned} \quad (4.6)$$

Since $a(t_i) > 1$, the above equation provides an upper bound to r_p when we set $a(t_i) = 1$. Using (2.2), it follows that

$$r_p \leq 7.8 \times 10^{60} \ell_{\text{Pl}} + 5 \times 10^{59} \ell_{\text{Pl}} \approx 8 \times 10^{60} \ell_{\text{Pl}}. \quad (4.7)$$

This is smaller than r_o by a factor of 3.75 [see (2.13)] and therefore the results presented in Sec. III A 3 describe the expected distribution of the circle sizes up to errors of a few percent. In particular, the largest circle possible is one where $\sin^{-1} \theta_o = r_p/r_o$ and this corresponds to⁷

$$\theta_o^{\text{max}} \approx 15^\circ. \quad (4.8)$$

In addition, since in the limiting case $r_o \approx 3.75r_p$ (i.e. the largest possible r_p) we have $d \approx r_o$, Eq. (3.37) simplifies to

$$\delta\theta_o \approx \frac{1}{3000 \sin \theta_o}. \quad (4.9)$$

It follows that in this case the width of the circles could be detected, but only for small circles whose angular radius is less than approximately 3° . This will of course slightly vary depending on the exact relation between d and r_o .

Therefore, in CCC with the choice of the conformal mapping chosen above, any circular imprints in the CMB would have at most an angular radius of approximately 15° and whose relation between the width and radius is given by (4.9).

Alternatively, one could choose a different conformal mapping where the conformal factor differs by a factor α in order to obtain, e.g., a different maximal radius for the circles. In this case the first term in (4.7) will be multiplied by α and this will change the size distribution of the circles as well as the maximal circle size possible. It will also change the relation between the width and the size of the circles, although (3.37) will still hold so long as $\alpha < 10^{11}$. However, the conformal mapping that we used in this section appears to us to be the most natural one and a different choice may be difficult to motivate.

B. The Ekpyrotic Universe

The ekpyrotic universe is a cyclic cosmological model motivated by string theory [11–13]. The idea is that the classical big bang corresponds to a collision between two branes and that the accelerated expansion of the universe at late times is due to the potential energy between the two branes being slightly larger than zero when the separation is large. This period of accelerated expansion lasts for a very long time and ensures that the entropy density and black hole number density both become negligible before the big-crunch/big-bang transition and thus set appropriate “initial conditions” for the beginning of the next cosmological

⁷ Note that in [7] the maximum angular radius allowed is given as 30° rather than the 15° we find.

epoch. The field that determines the distance between the two branes is modelled by a scalar field with a potential that satisfies certain requirements, see [11–13] for further details.

Since the black hole number density in the universe at late times is very low, any supermassive black hole collisions must happen around $\rho = \rho(t_{\text{now}})$ in the previous epoch and thus $a(t_i) \approx 1$. It follows that, as in CCC, the observed width of any circles in the CMB would be due to the width of the CMB sphere and Eq. (3.37) holds.

In addition, given a specific potential for the scalar field, it is also possible to derive an approximate value for r_p . A portion of the calculation is very similar to the one performed in the previous section on CCC: first there is a very long phase of accelerated expansion which can be modelled by a small cosmological constant and then, after the big-crunch/big-bang transition, there is a radiation-dominated phase up until the point where the last scattering surface forms. Therefore, the two terms that contribute to the CCC model also contribute for the ekpyrotic universe.

However, we must also include the contracting phase of the ekpyrotic cosmology in our calculation where the universe collapses from a scale factor which is very large to one that is zero on a time-scale of $\Lambda^{-1/2}$, where $\Lambda \approx 10^{-122} \ell_{\text{Pl}}^{-2}$ is the observed value of the cosmological constant. The main part of this collapse is potential-dominated and we can approximate the scale factor by

$$a(t) = a_{\text{max}}^{1-\sqrt{\Lambda}(t-t_{\text{con}})}, \quad (4.10)$$

where t_{con} is the time at which the universe starts to contract and a_{max} is the maximal scale factor reached. It is easy to see that this contracting phase contributes to r_p a term given by⁸

$$\int_0^{\Lambda^{-1/2}} \frac{dt}{a_{\text{max}}^{1-\sqrt{\Lambda}t}} = \frac{1}{\sqrt{\Lambda} \ln a_{\text{max}}}, \quad (4.11)$$

which is negligible compared to terms of the order of $10^{60} \ell_{\text{Pl}}$ since we expect a_{max} to be several orders of magnitude greater than 1. Therefore, this phase of the evolution of the universe contributes a term which is negligible when compared to the two other terms that were present in CCC [see (4.7)] and thus

$$r_p \leq 8 \times 10^{60} \ell_{\text{Pl}}. \quad (4.12)$$

This is the same result as in the CCC model and the observational predictions of the models are therefore identical: the largest circle should have a radius of approximately 15° and the relation between the size and the width of the circles should be observable (assuming the circles are indeed seen) and have the form of, e.g.,

$$\delta\theta_o \approx \frac{1}{3000 \sin \theta_o}, \quad (4.13)$$

for the limiting case of $r_p = \frac{4}{15} r_o$.

⁸ In our calculations we have neglected the portion of the evolution very close to the transition point $a(t=0) = 0$ which is dominated by the kinetic energy of the scalar field. However, this part of the universe's evolution is incredibly short and does not significantly contribute to the value of r_p .

C. Loop Quantum Cosmology without Inflation

Loop quantum cosmology (LQC) is the result of applying the methods of loop quantum gravity to simple space-times such as the homogeneous and isotropic FLRW models [14–16]. For our purposes, the most important feature is that in LQC the universe undergoes a quantum bounce when the scalar curvature approaches the Planck scale. The pre- and post-bounce phases are extremely well approximated by classical contracting and expanding cosmologies respectively so long as the scalar curvature remains far from the Planck regime.

In particular, the Friedmann equation is modified due to quantum geometry effects and, when the matter field can be described as a perfect fluid, it becomes [17]

$$\left(\frac{\dot{a}}{a}\right)^2 = \frac{8\pi G}{3}\rho\left(1 - \frac{\rho}{\rho_c}\right), \quad (4.14)$$

where the dot denotes differentiation with respect to the proper time t and $\rho_c \approx 0.41\rho_{\text{Pl}}$ is the critical matter energy density where the bounce occurs. One can see that quantum geometry effects provide a repulsive force when the matter energy density reaches the Planck scale. Also note that the dynamics are symmetric around the bounce point where $\rho = \rho_c$.

The matter fields behave in the same way as in standard cosmology, e.g., for a radiation fluid

$$\rho = \frac{\rho_o}{a(t)^4}, \quad (4.15)$$

where ρ_o is a constant to be determined by the initial conditions. For the initial conditions given at recombination in (2.3) and (2.4),

$$\rho_o = 10^{-127} \rho_{\text{Pl}}. \quad (4.16)$$

One can consider an LQC model which began in the distant past as a large, approximately homogeneous universe that contracted, bounced and expanded to the universe we see today without undergoing a period of slow-roll inflation. Whilst such a model would have several important difficulties that would need to be addressed—such as why the bounce was approximately homogeneous, why the perturbations are almost scale invariant, etc.—here we shall ignore these issues and simply study the properties of the circles that would be produced in this model.

We will now assume that, since there is no inflation, the universe is radiation-dominated so long as the energy density is greater than $\rho_{\text{CMB}} = 10^{-115}\rho_{\text{Pl}}$, i.e., the energy density that recombination occurs at. It is then possible to use (4.15) in order to solve the modified Friedmann equation and this gives

$$a(t) = \left(\frac{32\pi G\rho_o}{3}t^2 + \frac{\rho_o}{\rho_c}\right)^{1/4}. \quad (4.17)$$

It is clear that the scale factor is strictly greater than zero at all times—there is no singularity—and also that it is time symmetric around the bounce point at $t = 0$.

We will assume that any astrophysical event that could be a source for a circle seen in the CMB would have to occur at relatively low energy densities and in particular at a time when the energy density is less than ρ_{CMB} . We are choosing this cutoff as we are assuming

that the strength of any major collisions that occur at energies where there exists a photon, proton and electron plasma would be strongly damped by this plasma⁹.

Since we are only considering collisions that occur when $\rho < \rho_{\text{CMB}}$, it follows that $a(t_i) > 10^{-3}$ and therefore the width of the circles is dominated by the contribution from δr_o and we can use (3.37).

It is also possible to calculate a minimal value for r_p by assuming that the collision happens just as the plasma is forming in the pre-bounce phase. One would of course expect most supermassive black hole collisions to occur much earlier than the time reverse of recombination in the pre-big-bang epoch, but this limiting event will provide a lower bound for r_p :

$$r_p \geq c \int_{-t_{\text{CMB}}}^{t_{\text{CMB}}} \frac{dt}{a(t)}. \quad (4.18)$$

Using (4.17) to evaluate the expression above, one finds that

$$r_p \geq 10^{60} \ell_{\text{Pl}}, \quad (4.19)$$

which is smaller than r_o by a factor of 30. However, unlike for CCC and the ekpyrotic universe, this is a *lower bound* and it is easy to obtain r_p 's which are significantly larger by simply considering collisions that occur at times much earlier than when the plasma forms. Thus within this model, it is possible to obtain both small (when $r_p \ll r_o$) and large (when $r_p \geq r_o$) circles. However, in all cases smaller circles should be thicker (assuming their width is observed) due to the selection effect due to the $\sin \theta_o$ in the denominator in Eq. (3.35).

D. Loop Quantum Cosmology with Inflation

If one introduces an inflaton field into an LQC model, the quantum bounce will be followed by a phase of standard slow-roll inflation. In addition to resolving the classical singularity, LQC naturally sets the initial conditions for slow-roll inflation [18, 19]. An important point here is that since the inflaton is not a perfect fluid, $a(t)$ is not necessarily symmetric around the bounce point: it is possible to have a long period of slow-roll inflation after the bounce without a corresponding period of slow-roll deflation before the bounce and vice versa. Of course, a symmetric evolution in which there is exactly the same amount of deflation and inflation is also a solution, however the likelihood of this occurring is very low.

In the following we will assume that there are N_{asym} efoldings of asymmetry between the slow-roll deflationary and inflationary phases, i.e., that $N_{\text{inf}} - |N_{\text{def}}| = N_{\text{asym}}$ where N_{inf} is the number of efoldings of slow-roll inflation after the bounce and N_{def} is the number of efoldings of slow-roll deflation before the bounce.

We will also denote the number of efoldings of super-inflation/ deflation as N_{LQC} , which occurs immediately around the bounce point, is approximately symmetric and is typically 2 or 3. Then the scale factor at the end of slow-roll inflation is approximately $a(t_{\text{end}}) \approx a(t=0) e^{N_{\text{LQC}} + N_{\text{inf}}}$, whilst the scale factor at the time slow-roll deflation began is $a(t_{\text{beg}}) \approx$

⁹ Although it might be possible for a supermassive black hole collision to release a lot of energy even if the collision has been damped by the presence of a plasma, an investigation along these lines is outside of the scope of this paper. Nonetheless, if this were to happen, the circle size would be very small as in this case $r_p \leq 10^{60} \ell_{\text{Pl}} \ll r_o$ and $\theta_o^{\text{max}} \leq 1/30$ rad.

$a(t=0) e^{N_{\text{LQC}} + |N_{\text{def}}|}$. Thus, in this model the dynamics of the scale factor can be highly asymmetric if N_{inf} and N_{def} are significantly different.

If we estimate the amount of expansion that the universe underwent after slow-roll inflation (i.e., during standard cosmology) to be approximately 3×10^{28} [10], then we have

$$a(t=0) \approx e^{-65.6 - N_{\text{inf}} - N_{\text{LQC}}}, \quad (4.20)$$

where recall $a(t_{\text{now}}) = 1$.

Defining $a(t_i)$ to have occurred x -foldings before the beginning of the slow-roll deflation period, we have

$$a(t_i) \approx e^{x + |N_{\text{def}}| + N_{\text{LQC}}} a(t=0). \quad (4.21)$$

In this model, it is possible for δr_p 's contribution to the width be significant if $x < N_{\text{asym}} + 40$. Typically, we would expect x to be at least 65.6 in order for the universe to be sufficiently diluted so that any black hole collisions would not be significantly damped and, for this to occur and for the inequality to hold, we must have an extremely asymmetric solution. In this case, the contribution of δr_p will no longer be negligible and it will be necessary to use (3.35) in order to describe the width of the circles.

It is possible to obtain a strong lower bound for r_p by studying the contribution due to the inflationary phase which is given by

$$c \int_{t_{\text{start}}}^{t_{\text{inf}}} \frac{dt}{a(t)} \approx \frac{1}{a(t_{\text{start}}) H_{\text{inf}}} \approx 10^{64} \ell_{\text{Pl}}, \quad (4.22)$$

where $a(t_{\text{start}}) \approx 10^{-58}$ is the scale factor at the beginning of inflation having assumed 70 efoldings and $H_{\text{inf}} \approx 10^{-6} \ell_{\text{Pl}}^{-1}$ is the Hubble rate during inflation.

It then follows that, since this is just one of several contributions to r_p ,

$$r_p \geq 10^{64} \ell_{\text{Pl}}, \quad (4.23)$$

which is clearly significantly larger than r_o .

Since $r_p \gg r_o$, it follows that the relation between the width and the radius of the circles given in (3.35) can be simplified. First, since $r_p \gg r_o$ it follows that $\theta_p \ll 1$ and then by using the cosine rule,

$$r_p^2 + r_o^2 - d^2 = 2r_p r_o \cos(\pi - \theta_o - \theta_p) \quad (4.24)$$

$$\approx 2r_p r_o \cos(\pi - \theta_o). \quad (4.25)$$

This allows us to express the width as

$$\delta\theta_o \approx \frac{c\delta t}{a(t_i)r_o \sin\theta_o} + \frac{\cot(\theta_o)}{100}, \quad (4.26)$$

and therefore we would expect to be able to detect the width of small circles. As for the other models studied here, smaller circles are expected to be thicker.

An important point here is that the results obtained for LQC with inflation depend solely on the presence of the inflationary phase in our current epoch as the properties of the pre-big-bang epoch (apart from its existence) are washed out by inflation. Therefore, the conclusions obtained in this section hold for all pre-big-bang cosmological models that include inflation. For these models, we should expect to see circles whose width is greater for smaller circles and their average angular radius should be 57° with a variance of $(22^\circ)^2$.

V. DISCUSSION

For many of the pre-big-bang cosmological models that are currently being studied, it is still not entirely clear how inhomogeneities propagate from the pre-big-bang era to the present epoch. Nonetheless, if a pre-big-bang phase does indeed provide the seeds for the inhomogeneities we see today in our universe, there exists the possibility of observing some signatures of the pre-big-bang era in our universe and, in particular, in the CMB.

Of course, depending on the specific pre-big-bang cosmological model, there may exist several signatures of the previous eon that one could find in the CMB. However, one particular potential signature common to several models (and which is relatively easy to search for) is the presence of circles with abnormally low temperature variance in the CMB. Such circles would be due to gravitational waves produced by supermassive black hole collisions (or other extremely energetic events) from the pre-big-bang era. Even though the mechanism which allows for the transfer of the correlations from the gravitational waves to the last scattering surface is not clear, it is possible to predict some of the geometric properties of these circles given a pre-big-bang cosmological model. It is worth noting that different types of circles, such as abnormally high or low temperature circles due to the Sachs-Wolfe effect, could potentially also exist in the CMB [8] and the results presented here hold for the geometric properties of these other types of circles as well.

An important point is that we assume that quantum gravity corrections to the size of circles in the CMB will be negligible and therefore we only calculate the dominant classical contributions. Nonetheless, quantum gravity plays a central role as it provides the bridge between the pre- and post-big-bang epochs: without it, there would be no way for the gravitational wave pulse to travel from one epoch to the other as there would necessarily be a singularity. Of course, it would be interesting to see how the pulse might be affected by quantum gravity effects near the transition point, but this question cannot be answered until the full dynamics of quantum cosmology are understood.

In this paper, we have obtained a probability distribution for the size of the circles, studied the expected separation between concentric circles and predicted the width of the circles. Note that this analysis is not complete: for example, we make no claims regarding the total number of circles that one would expect to see in the CMB. Nonetheless, by studying four specific cosmological models which have a pre-big-bang epoch—conformal cyclic cosmology, ekpyrotic cosmology and loop quantum cosmology with and without inflation—we have shown that the probability distribution of the circle size varies from one cosmological model to another and this could potentially be used in order to differentiate between cosmological models based upon careful observations of the CMB. We must stress that we are not predicting the presence of these circles in the CMB. Rather, what we have done is to show how, assuming the circles are present, their geometric properties would differ from one cosmological model to another.

In particular, in conformal cyclic cosmology and the ekpyrotic universe, one would expect there to be only very small circles with an angular radius of at most 15° , while in LQC without inflation one would expect larger circles as well whereas for LQC with inflation (and also all other pre-big-bang models that have an inflationary era), one should expect a distribution of large circles with an average angular radius of 57° .

Also, in all of these models one expects the width and the radius of the circles to be related. The relations presented in Sec. IV describing the ring width for each cosmological model are often given for a specific value of r_p , but they can easily be generalized. In fact,

these relations offer a simple way to test whether the circles found in [1] are due to extremely energetic events in a pre-big-bang epoch or not: if the smaller circles are also wider, this would provide strong evidence in support of the viewpoint presented in [1]. If not, then it seems more likely that the circles are simply statistical flukes or, perhaps, are due to a completely different mechanism. If the circles described in [1] are indeed imprints from pre-big-bang events, their geometric properties will give significant insight into the dynamics of the pre-big-bang era of our universe and also the nature of the quantum gravity effects that were undoubtedly important in the early universe.

Acknowledgments

We would like to thank Alexey Bobrick, Lee Sam Finn, Vahe G. Gurzadyan, Nathan Johnson-McDaniel, Roger Penrose, Carlo Rovelli, David Sloan and James Zibin for helpful discussions. This work is supported in part by the NSF grant PHY0854743, Le Fonds québécois de la recherche sur la nature et les technologies, the George A. and Margaret M. Downsbrough Endowment and the Eberly research funds of Penn State.

-
- [1] V. G. Gurzadyan and R. S. Penrose, “Concentric circles in WMAP data may provide evidence of violent pre-Big-Bang activity,” [arXiv:1011.3706 \[astro-ph.CO\]](#), (2010).
 - [2] I. K. Wehus and H. K. Eriksen, “A search for concentric circles in the 7-year WMAP temperature sky maps,” [arXiv:arXiv:1012.1268 \[astro-ph.CO\]](#), (2010).
 - [3] A. Moss, D. Scott and J. P. Zibin, “No evidence for anomalously low variance circles on the sky,” [arXiv:1012.1305 \[astro-ph.CO\]](#), (2010).
 - [4] A. Hajian, “Are There Echoes From The Pre-Big Bang Universe? A Search for Low Variance Circles in the CMB Sky,” [arXiv:1012.1656 \[astro-ph.CO\]](#), (2010).
 - [5] V. G. Gurzadyan and R. S. Penrose, “More on the low variance circles in CMB sky,” [arXiv:1012.1486 \[astro-ph.CO\]](#), (2010).
 - [6] V. G. Gurzadyan and R. Penrose, [arXiv:1104.5675 \[astro-ph.CO\]](#).
 - [7] R. Penrose, *Cycles of time: An extraordinary new view of the universe*, The Bodley Head, (2010).
 - [8] J. P. Zibin, private communication.
 - [9] S. Weinberg, *Cosmology*, Oxford University Press, (2008).
 - [10] P. Peter, J.-P. Uzan, *Primordial Cosmology*, Oxford University Press, (2009).
 - [11] J. Khoury, B. A. Ovrut, P. J. Steinhardt and N. Turok, “The Ekpyrotic universe: Colliding branes and the origin of the hot big bang,” *Phys. Rev.* **D64**, 123522 (2001).
 - [12] P. Steinhardt and N. Turok, “Cosmic evolution in a cyclic universe,” *Phys. Rev.* **D65**, 126003 (2002).
 - [13] P. Steinhardt and N. Turok, “A cyclic model of the universe,” *Science* **296**, 1436-1439 (2002).
 - [14] A. Ashtekar, T. Pawłowski and P. Singh, “Quantum Nature of the big bang: Improved dynamics,” *Phys. Rev.* **D74**, 084003 (2006).
 - [15] M. Bojowald, “Loop quantum cosmology,” *Liv. Rev. Rel.* **8** (2005).
 - [16] A. Ashtekar, “Singularity Resolution in Loop Quantum Cosmology: A Brief Overview,” *Jour. Phy. Conf. Ser.* **189**, 012003 (2009).

- [17] V. Taveras, “LQC corrections to the Friedmann equations for a universe with a free scalar field,” *Phys. Rev.* **D78**, 064072 (2008).
- [18] A. Ashtekar and D. Sloan, “Loop quantum cosmology and slow roll inflation,” *Phys. Lett.* **B694**, 108 (2010).
- [19] A. Ashtekar and D. Sloan, “Probability of Inflation in Loop Quantum Cosmology,” [arXiv:1103.2475](https://arxiv.org/abs/1103.2475) [gr-qc], (2011).